




Letters

A Simplified Three-Order Small-Signal Model for Capacitive Power Transfer System Using Series Compensation

Chaoqun Qi, Guangce Zheng, *Student Member, IEEE*, Yu Liu, *Senior Member, IEEE*, Junrui Liang , *Senior Member, IEEE*, Haoyu Wang , *Senior Member, IEEE*, and Minfan Fu , *Senior Member, IEEE*

Abstract—Capacitive power transfer is promising for high-efficiency wireless charging. A small-signal model is required to evaluate the system stability under different control approaches. This letter focuses on the modeling and simplification of the high-order system using series compensation. Based on the extended describing function method, this letter proposes a series of model transformation and approximation to effectively reduce the circuit order of the resonant tank. The number of resonant components is reduced from ten to two. Combining with the inverter and rectifier model, a third-order equivalent circuit model is first derived for the whole system with clear physical meaning and explicit transfer function. The experiment results show the model is accurate up to 1/5 of the switching frequency.

Index Terms—Capacitive power transfer, extended describing function, series compensation, small signal model.

I. INTRODUCTION

CAPACITIVE power transfer (CPT) is promising for the mid-range high-efficiency power transfer. Compared to the inductive power transfer (IPT), a CPT system has several unique benefits: such as no eddy-current loss for the surrounding conductive objects and low cost for coupler fabrication. Currently, the main research focuses for CPT include the coupler structure design, steady-state model, parameter design, compensation network, and application-driven system solutions [1], [2],

Manuscript received 10 November 2022; revised 11 December 2022 and 14 January 2023; accepted 2 February 2023. Date of publication 7 February 2023; date of current version 10 March 2023. This work was supported in part by National Natural Science Foundation of China under Grant 52007120. (Corresponding author: Minfan Fu.)

Chaoqun Qi is with the School of Information Science and Technology, ShanghaiTech University, Shanghai 201210, China, and with the Shanghai Advanced Research Institute, Chinese Academy of Sciences, Shanghai 201210, China, and with the Shanghai Institute of Microsystem and Information Technology, Chinese Academy of Sciences, Shanghai 200050, China, and also with the University of Chinese Academy of Sciences, Beijing 100049, China (e-mail: qichq@shanghaitech.edu.cn).

Guangce Zheng, Yu Liu, Junrui Liang, Haoyu Wang, and Minfan Fu are with the School of Information Science and Technology, ShanghaiTech University, Shanghai 201210, China, and also with the Shanghai Engineering Research Center of Energy Efficient and Custom AI IC, Shanghai 201210, China (e-mail: zhenggc@shanghaitech.edu.cn; liuyu@shanghaitech.edu.cn; liangjr@shanghaitech.edu.cn; wanghy@shanghaitech.edu.cn; fumf@shanghaitech.edu.cn).

Color versions of one or more figures in this article are available at <https://doi.org/10.1109/TPEL.2023.3243134>.

Digital Object Identifier 10.1109/TPEL.2023.3243134

TABLE I
MODELING COMPARISON OF S-S WPT SYSTEMS

Compensation	S-S IPT			S-S CPT	
	[8]	[9]	[10]	[7]	This paper
Literature					
Order of the model	4	4	5	5	3
Equivalent circuit model	×	✓	✓	✓	✓
Explicit transfer function	×	×	✓	×	✓

[3]. The active circuit (i.e., inverter or rectifier) and modulation approaches of IPT systems are also applicable for the CPT systems [4]. All these achievements are meaningful to optimize the system steady-state performance.

As a typical dc/dc resonant converter, a CPT system also incorporates a feedback control to stabilize the output. For this purpose, small-signal models are indispensable for control parameter optimization and stability analysis. In the past years, the modeling approaches for resonant converters have been successfully extended to IPT systems [5], [6]. Based on similar fundamental assumptions, the major differences of these paper are the topology, modulation approach, and the simplification method. In theory, similar modeling concept and technique are also valid for a CPT system. Based on the IPT model method in [6], a fifth-order equivalent circuit model is developed for a S-S compensated CPT system [7]. However, the explicit transfer function is not given and there is no experimental verification. A comparison of previous works about S-S WPT modeling is given Table I. The model order is higher than three. There still lacks a detailed discussion on the small-signal model for a S-S CPT system.

This letter is devoted to the small-signal model of a S-S CPT system based on extended describing function (EDF) method. At the fixed resonant frequency, the S-S system is able to offer a load-independent output current and achieve zero phase angle operation. The modeling starts from a capacitive coupler using induced current source (ICS) model, which is convenient to absorb the additional shunt capacitors. The small-signal model transformation between a capacitor and an inductor is proposed for the simplification of both parallel and series branch. A novel inductor-to-capacitor transformation is first used to simplify the

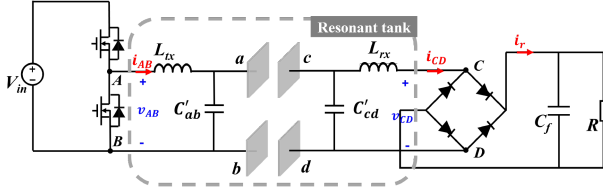


Fig. 1. CPT system using S-S compensation.

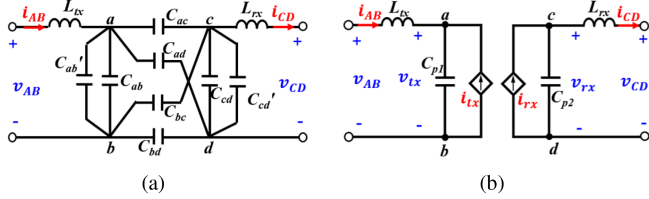


Fig. 2. Resonant tank model. (a) Using six-capacitor model. (b) Using ICS model.

parallel branch. Through the proposed circuit transformation, the number of resonant components is reduced from ten to two from the small-signal perspective. Finally, the whole system model is built by the circuit synthesis of the proposed tank model and the models of inverter and rectifier. The proposed model transformation and simplification concept are general and particularly attractive for CPT systems, and they can be directly applied for other CPT systems with different compensations.

II. EDF-BASED MODELING

A. Coupler Model Under Steady State

The CPT system configuration using SS compensation is shown in Fig. 1. It usually includes an inverter, a middle resonant tank, and a rectifier. In the resonant tank, there are four conductive plates (noted as a, b, c, and d) to build the capacitive coupler, and two series inductors (i.e., L_{tx} and L_{rx}) are added for compensation. Two shunt capacitors C'_{ab} and C'_{cd} are needed to reduce the required compensation inductance.

The circuit model of the resonant tank is shown in Fig. 2(a). There are six structure mutual capacitance, i.e., C_{ab} , C_{cd} , C_{ac} , C_{bd} , C_{ad} , and C_{bc} , and four additional components, i.e., L_{tx} , L_{rx} , C'_{ab} , and C'_{cd} . v_{AB} , v_{CD} , i_{AB} , and i_{CD} represent the terminal voltage and current of the resonant tank, i_r represents the output current of rectifier. It is challenging to directly build the small signal model for this ten-components circuit.

The ICS model is proposed in [11] for steady-state analysis, which would serve as the start point for the model simplification. As shown in Fig. 2(b), all the middle eight capacitors are equivalently represented by a pair of shunt capacitors (i.e., C_{p1} and C_{p2}) and a pair of ICS (i.e., i_{tx} and i_{rx}). The final equivalent shunt capacitors are derived as

$$\begin{cases} C_{p1} = C'_{ab} + C_{ab} + \frac{(C_{ac} + C_{ad}) \times (C_{bc} + C_{bd})}{C_{ac} + C_{ad} + C_{bc} + C_{bd}} \\ C_{p2} = C'_{cd} + C_{cd} + \frac{(C_{ac} + C_{bc}) \times (C_{ad} + C_{bd})}{C_{ac} + C_{ad} + C_{bc} + C_{bd}} \end{cases} \quad (1)$$

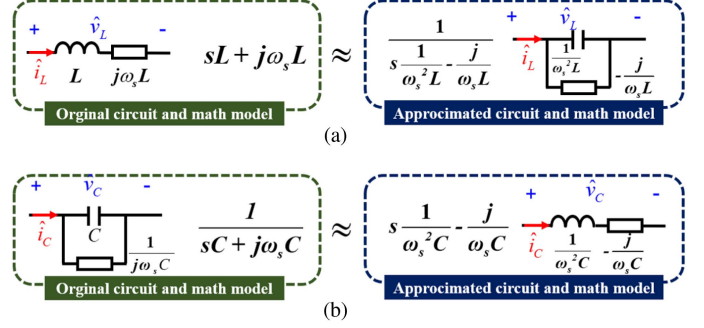


Fig. 3. Small-signal model transformation between a capacitor and inductor. (a) From inductor to capacitor. (b) From capacitor to inductor.

An equivalent mutual capacitance is derived as

$$C_{pm} = \frac{C_{ac}C_{bd} - C_{ad}C_{bc}}{C_{ac} + C_{ad} + C_{bc} + C_{bd}}. \quad (2)$$

It helps define the ICS as functions of coupler terminal voltage v_{tx} (TX-side) and v_{rx} (RX-side), i.e.,

$$\begin{cases} i_{tx}(t) = C_{pm} \frac{dv_{rx}(t)}{dt} \\ i_{rx}(t) = C_{pm} \frac{dv_{tx}(t)}{dt} \end{cases} \quad (3)$$

B. Model Simplification of the Resonant Tank

The model of the resonant tank needs to consider the small signal behavior of each components, i.e., the inductor, the capacitor, and the induced source. In [6], the equivalent small-signal model for an inductor and a capacitor have been discussed. Assume ω_s is the angular form of the switching frequency f_s , and s is the perturbation frequency for the small signal. As shown in the left of Fig. 3(a), the inductor model has a frequency-dependent (i.e., s -dependent) component (sL) and a frequency-independent (i.e., s -independent) impedance ($j\omega_s L$) to form a series branch. The capacitor model is represented by a parallel branch, i.e., C and $1/(j\omega_s C)$ (refer to the left of Fig. 3(b)).

When the perturbation frequency $s \ll \omega_s$, it has $\frac{s^2}{\omega_s^2} + 1 \approx 1$, using this approximation, it has

$$\frac{\hat{v}_C}{\hat{i}_C} = \frac{1}{sC + j\omega_s C} = \frac{s - j\omega_s}{\left(\frac{s^2}{\omega_s^2} + 1\right)\omega_s^2 C} \approx s \frac{1}{\omega_s^2 C} - \frac{j}{\omega_s C}. \quad (4)$$

The above derivation shows the capacitor model can be approximately represented as an inductor form. Such a capacitor-to-inductor (C2L) model transformation was proposed in [5], which is helpful to simplify the series resonant tank [see Fig. 3(b)]. It means when the components of a series branch are all represented by their inductor form, the circuit order is reduced due to the model combination. In a reverse manner, an inductor-to-capacitor (L2C) transformation is proposed in this letter based on the following approximation [see Fig. 3(a)]:

$$\frac{\hat{v}_L}{\hat{i}_L} = sL + j\omega_s L \approx \frac{1}{s \frac{1}{\omega_s^2 L} - \frac{j}{\omega_s L}}. \quad (5)$$

This model transformation is powerful in the model simplification for parallel resonance.

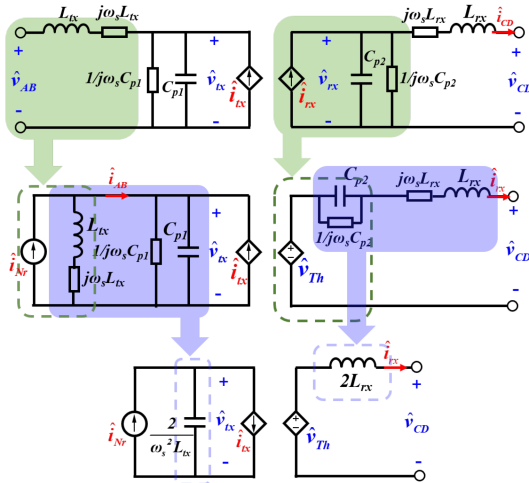


Fig. 4. Resonant tank simplification.

In order to model the induced source, the fundamental components of the state variables are represented by their complex signal forms. Assume $i_{tx}(t) \approx I_{tx}e^{j\omega_s t}$, $i_{rx}(t) \approx I_{rx}e^{j\omega_s t}$, $v_{tx}(t) \approx V_{tx}e^{j\omega_s t}$, and $v_{rx}(t) \approx V_{rx}e^{j\omega_s t}$. Apply small perturbation to v_{tx} , v_{rx} , i_{tx} , and i_{rx} in (3), it has

$$\begin{cases} i_{tx}(t) \approx (\bar{I}_{tx} + \hat{i}_{tx}) e^{j\omega_s t} = C_{pm} \frac{d(\bar{V}_{rx} + \hat{v}_{rx}) e^{j\omega_s t}}{dt} \\ i_{rx}(t) \approx (\bar{I}_{rx} + \hat{i}_{rx}) e^{j\omega_s t} = C_{pm} \frac{d(\bar{V}_{tx} + \hat{v}_{tx}) e^{j\omega_s t}}{dt} \end{cases} \quad (6)$$

The small signal model for the ICS is derived as

$$\begin{cases} \hat{i}_{tx} = \hat{v}_{rx} C_{pm}(s + j\omega_s) \\ \hat{i}_{rx} = \hat{v}_{tx} C_{pm}(s + j\omega_s). \end{cases} \quad (7)$$

By synthesizing the small-signal model of each basic component, the model of the whole resonant tank is generated as shown in Fig. 4 (refer to the top circuit). Since the original circuit has series and parallel branches at both sides, such a high-order system is not convenient for explicit model derivation. This letter would fully use the L2C and C2L transformation of Fig. 3 and the well-known circuit theory for model simplification.

In Fig. 4, the green area of the top model is equivalently transformed to corresponding part of the middle model. This transformation is based on the Norton's and Thevenin's theory, i.e.,

$$\begin{cases} \hat{i}_{Nr} = \hat{v}_{AB} / [L_{tx}(s + j\omega_s)] \\ \hat{v}_{Th} = \hat{v}_{rx} = \hat{i}_{rx} / [C_{p2}(s + j\omega_s)]. \end{cases} \quad (8)$$

In a typical CPT system, the capacitance is usually pF level and the inductance is μH level. Hence, the impedance of the capacitor is much higher than that of the inductor in the low-frequency region. Thus, when the low-frequency perturbation is applied, the resonant tank output current \hat{i}_{CD} can be approximated as \hat{i}_{rx} (refer to the output terminal of Fig. 4). The next step is to simplify the blue part of the middle model. For the TX-side circuit, the blue part is a typical parallel resonant tank, and a L2C transformation is applied. For the RX side, a C2L transformation is used for the series branch. When the system operates at the fixed resonance frequency, i.e., working like a

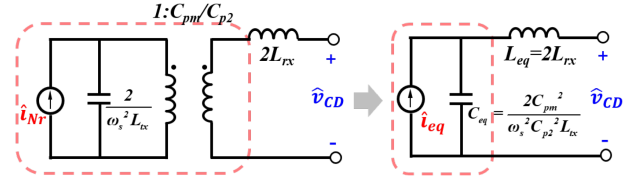


Fig. 5. Merging TX to RX.

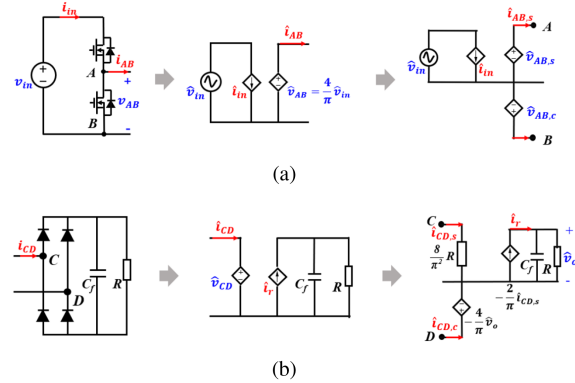


Fig. 6. Small signal model for inverter and rectifier. (a) Decomposition of inverter model. (b) Decomposition of rectifier model.

constant current (CC) source, it is able to further simply the model as shown in the bottom of Fig. 4. Note that the proposed simplification is invalid when frequency modulation is applied.

The further simplification is to deal with the induced source part in the bottom model of Fig. 4. Combining (7) and (8), it has

$$\hat{v}_{rx} = \frac{C_{p2}}{C_{p2}} \hat{v}_{tx}. \quad (9)$$

It means the two induced sources can be replaced by an ideal transformer as shown in the left of Fig. 5. Using the transformer, all the TX-side circuit is reflected to the RX side, and the final resonant tank model is shown in the right of Fig. 5, where

$$\begin{cases} \hat{i}_{eq} = \frac{C_{p2}}{C_{pm}} \hat{i}_{Nr} = \frac{C_{p2}}{(s + j\omega_s) C_{pm} L_{tx}} \hat{v}_{AB} \\ L_{eq} = 2L_{rx} \\ C_{eq} = 2C_{p2}^2 / (\omega_s^2 C_{pm}^2 L_{tx}). \end{cases} \quad (10)$$

The final tank model only contains an equivalent capacitor (C_{eq}), an equivalent inductor (L_{eq}), and a current source. Compared with the original tank model, the number of components is dramatically reduced, and model order is successfully reduced.

C. Whole System Model

The model of the whole system needs to consider the inverter and rectifier, which have been discussed in [6] and are reviewed in Fig. 6. Using the phase of v_{AB} as the reference, the model of the rectifier and the resonant tank need to be decomposed for system synthesis. When $s \ll \omega_s$, (10) is simplified as

$$\hat{i}_{eq} \approx C_{p2} \hat{v}_{AB} / (j\omega_s C_{pm} L_{tx}). \quad (11)$$

The inverter is decomposed into two orthogonal subcircuits (a sine part and a cosine part) in Fig. 6(a). Considering the fixed

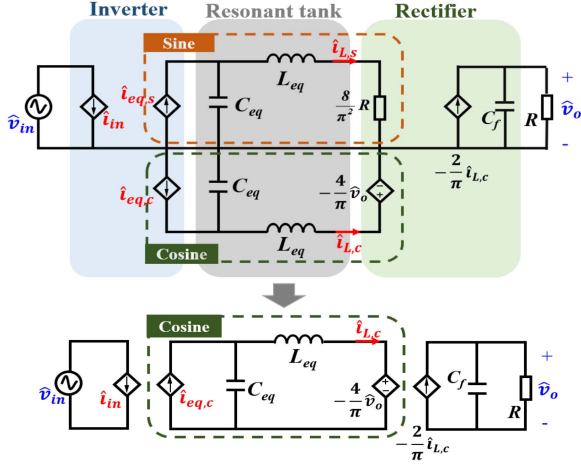


Fig. 7. Small signal model of a S-S CPT system.

phase difference between the inverter output (v_{AB}) and rectifier input (i_{CD}), the rectifier is decomposed as shown in Fig. 6(b).

The middle resonant tank model of Fig. 5 need to be decomposed in the same way, and then combined with the inverter and rectifier model. The overall system model is shown in the top of Fig. 7. According to (11), \hat{i}_{eq} is decomposed as

$$\begin{cases} \hat{i}_{eq,s} = 0 \\ \hat{i}_{eq,c} = -C_{p2}\hat{v}_{AB}/(\omega_s C_{pm} L_{tx}). \end{cases} \quad (12)$$

It is interesting to find that the output voltage is only affected by the current of the Cosine part. Since the Sine part is only coupled to the source but decoupled to the load, the final model is represented in the bottom of Fig. 7 (removing the sine part).

Using the equivalent circuit model of Fig. 7, many small-signal behaviors of a CPT system can be evaluated. For example, when the input voltage is regulated, the influence of the input perturbation can be evaluated through the voltage transfer function. Through the basic circuit theory, this voltage gain ($G_{vv} = \hat{v}_o/\hat{v}_{in}$) is derived as

$$G_{vv} = \frac{G_{dc}}{L_{eq}C_{eq}RC_f s^3 + L_{eq}C_{eq}s^2 + (RC_f + \frac{8}{\pi^2}RC_{eq})s + 1} \quad (13)$$

where

$$G_{dc} = 4RC_{p2}/(\pi^2\omega_s C_{pm} L_{tx}). \quad (14)$$

It is a three-order model with clear physical meaning. Such an explicit transfer function is convenient to design the parameters of a linear controller.

In (13), the output capacitance C_f (nF or μ F level) is usually much larger than the equivalent capacitance C_{eq} (pF level). Taking $C_f \gg C_{eq}$ into the dominator of (13), i.e., D_{vv} , it has

$$\begin{aligned} D_{vv} &\approx L_{eq}C_{eq}RC_f s^3 + L_{eq}C_{eq}s^2 + RC_f s + 1 \\ &= (L_{eq}C_{eq}s^2 + 1)(RC_f s + 1). \end{aligned} \quad (15)$$

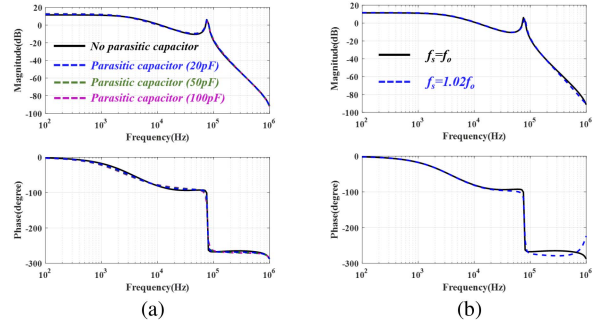


Fig. 8. Simulation verification. (a) Different diode junction capacitance. (b) Different switching frequency.

 TABLE II
 SETUP PARAMETERS

Parameter	C'_{ab}, C'_{cd}	C_{p1}, C_{p2}	L_{tx}, L_{rx}	C_f	P
Value	544 pF	645 pF	40.4 μ H	300 nF	30 W

Three poles exist in (15). The frequency of the single pole (f_{p1}) and conjugate poles (f_{p2}) are derived as

$$\begin{cases} f_{p1} = 1/(2\pi RC_f) \\ f_{p2} = \frac{1}{2\pi\sqrt{L_{eq}C_{eq}}} = C_{pm}\sqrt{\frac{L_{tx}}{2L_{rx}C_{p2}^2}}f_s. \end{cases} \quad (16)$$

It is obvious that f_{p1} is determined by C_f and R . f_{p2} is determined by L_{eq} and C_{eq} , i.e., the parameters of resonant tank. For example, the mutual capacitance C_{pm} would directly affect f_{p2} . When f_{p2} are much higher than f_{p1} , this system can further simplified as a single-pole one, whose transfer function is

$$G_{vv1} = G_{dc}/(RC_f s + 1). \quad (17)$$

For a practical system, the controller type needs to consider its bandwidth requirement. If the bandwidth is much lower than f_{p2} , the first-order model is sufficient to guide the controller design. An integrator and a lead compensator are sufficient. If the bandwidth is close to f_{p2} , the third-order model has to be used. A type-III (having three poles and two zeros) compensator is suggested.

A system is built in simulation with the same parameters as the final experiment. In the model, the diode junction capacitance are not included, whose effect is conveniently evaluated in simulation. When a small variation is applied to these capacitance, Fig. 8(a) shows there is almost no change in the system response and the model does not need to consider this parasitic. When the resonance frequency (f_o) is 1 MHz, the switching frequency should be higher to ensure zero-voltage switching. The response for different f_s is compared in Fig. 8(b). It shows a small frequency deviation will not affect the model accuracy.

III. MODEL VERIFICATION

A 1-MHz CPT system setup is built as shown in Fig. 9(a). All the system parameters are shown in Table II. The coupler parameters are measured by the impedance analyzer, i.e., shorting one terminal and reading the input impedance from

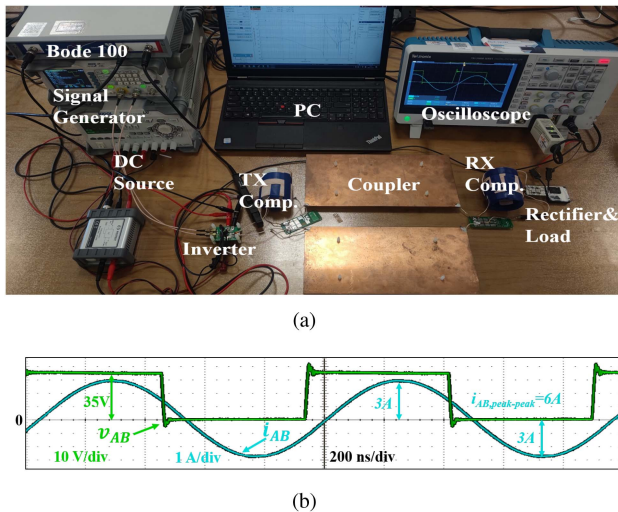


Fig. 9. Experiment setup. (a) Test platform. (b) Steady-state waveform.

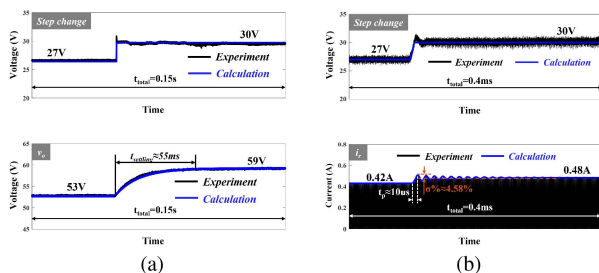


Fig. 10. Dynamic behaviors. (a) Final output voltage (after C_f). (b) Rectifier output current (before C_f).

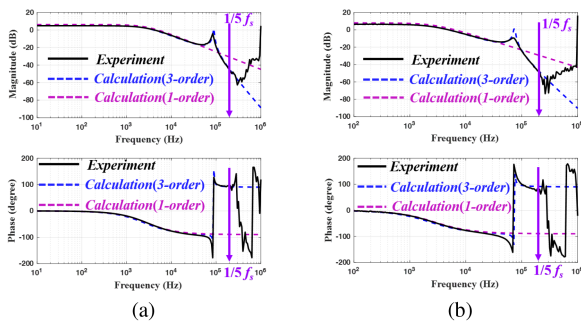


Fig. 11. Voltage gain. (a) $C_{pm} = 101.2$ pF. (b) $C_{pm} = 79.8$ pF.

another. The nominal resonance frequency is slightly less than the switching frequency to ensure the zero voltage switching of the inverter. The input voltage is 35 V and the output power is 30 W. The inverter output is shown in Fig. 9(b). When the input voltage experiences a step change, the dynamic behavior of output voltage (v_o) and the rectifier output current (i_r) are given in Fig. 10 to justify the model accuracy from time domain aspect.

Both the magnitude and phase of G_{vv} (three-order model) and G_{vv1} (one-order model) are given as shown in Fig. 11(a). The consistency between the model-based calculation and the real response clearly justifies the model accuracy. The third-order model is accurate up to one fifth of the switching frequency. It is sufficient to describe the low-frequency behaviors of the CPT

system. There exists a mismatch at the conjugate-pole position (around 100 kHz). This is due the influence of equivalent series resistors. The damping effect of the calculated response is not as clear as the real one. Fig. 11 also shows when the perturbation frequency is much lower than the conjugate-poles frequency, this system can be treated as a single-pole one. When the vertical distance increases, the mutual capacitance C_{pm} would drop from 101.2 to 79.8 pF. It equally means the coupling coefficient decreases from 0.15 to 0.12. The proposed model is still valid as shown in Fig. 11(b). In a coupling variation case, the range of C_{pm} should be measured, and then the system controller could define the worst case to guide the controller design.

IV. CONCLUSION

This letter mainly focuses on the small signal model for a S-S compensated CPT system from both circuit and math point of view. In order to simplify the high-order resonant tank, a new inductor-to-capacitor approximation is proposed and combined with the existing capacitor-to-inductor approximation. Through a series of model transformation, the complicated resonant tank can effectively simplify the resonance behavior from the small-signal perspective. Combing with the existing inverter and rectifier model, a third-order equivalent circuit model is generated and help explicitly derive the transfer function for the whole system. The measured results show the proposed model is accurate up to one fifth of the switching frequency.

REFERENCES

- [1] H. Zhang, F. Lu, H. Hofmann, W. Liu, and C. C. Mi, "Six-plate capacitive coupler to reduce electric field emission in large air-gap capacitive power transfer," *IEEE Trans. Power Electron.*, vol. 33, no. 1, pp. 665–675, Jan. 2018.
- [2] Y. Wu, Q. Chen, X. Ren, and Z. Zhang, "Efficiency optimization based parameter design method for the capacitive power transfer system," *IEEE Trans. Power Electron.*, vol. 36, no. 8, pp. 8774–8785, Aug. 2021.
- [3] S. Zang, Q. Zhu, L. Zhao, and A. P. Hu, "Capacitive power transfer system with integrated wide bandwidth communication," *IEEE Trans. Power Electron.*, vol. 37, no. 8, pp. 8805–8810, Aug. 2022.
- [4] J. Lian and X. Qu, "An LCLC-LC-compensated capacitive power transferred battery charger with near-unity power factor and configurable charging profile," *IEEE Trans. Ind. Appl.*, vol. 58, no. 1, pp. 1053–1060, Jan. 2022.
- [5] S. Tian, F. C. Lee, and Q. Li, "A simplified equivalent circuit model of series resonant converter," *IEEE Trans. Power Electron.*, vol. 31, no. 5, pp. 3922–3931, May 2016.
- [6] G. Zheng, P. Zhao, H. Li, and M. Fu, "Small-signal model of an inductive power transfer system using LCC–LCC compensation," *IEEE Trans. Ind. Appl.*, vol. 58, no. 1, pp. 1201–1210, Jan. 2022.
- [7] C. Qi, G. Zheng, Y. Yin, H. Li, and M. Fu, "Small-signal model for capacitive power transfer systems using series compensation," in *Proc. IEEE 31st Int. Symp. Ind. Electron.*, Anchorage, Alaska, USA, 2022, pp. 752–757.
- [8] Q. Deng et al., "Modeling and control of inductive power transfer system supplied by multiphase phase-controlled inverter," *IEEE Trans. Power Electron.*, vol. 34, no. 9, pp. 9303–9315, Sep. 2019.
- [9] S. Lee and S.-H. Lee, "DQ synchronous reference frame model of a series-series tuned inductive power transfer system," *IEEE Trans. Ind. Electron.*, vol. 67, no. 12, pp. 10325–10334, Dec. 2020.
- [10] G. Zheng, C. Qi, Y. Liu, J. Liang, H. Wang, and M. Fu, "Uniform and simplified small-signal model for inductive power transfer systems," *IEEE Trans. Power Electron.*, vol. 38, no. 2, pp. 2709–2719, Feb. 2023.
- [11] H. Zhang, F. Lu, H. Hofmann, W. Liu, and C. C. Mi, "A four-plate compact capacitive coupler design and LCL-compensated topology for capacitive power transfer in electric vehicle charging application," *IEEE Trans. Power Electron.*, vol. 31, no. 12, pp. 8541–8551, Dec. 2016.